ELSEVIER

Journal of Petroleum Science and Engineering 21 (1998) 15–26

JOURNAL OF PETROLEUM SCIENCE & ENGINEERING

Pressure buildup analysis of gas wells with damage and non-Darcy flow effect

Ibrahim S. Nashawi [a,*], Ahmed A. Elgibaly [a], Reyadh A. Almehaideb [b,1]

[a] *Department of Petroleum Engineering, College of Engineering and Petroleum, Kuwait University, P.O. Box 5969, Safat 10360, Kuwait*
[b] *Department of Chemical and Petroleum Engineering, College of Engineering, U.A.E. University, P.O. Box 17555, Al-Ain, United Arab Emirates*

Received 29 July 1997; revised 22 April 1998; accepted 22 April 1998

Abstract

This paper presents a technique to analyze pressure buildup test data of gas wells with damage and non-Darcy skin effect. This technique allows the analyst to estimate reservoir permeability and mechanical and rate-dependent skin factors directly by using 2 analysis plots. Formation permeability and rate-dependent skin are obtained from the slope and the intercept of the first plot, respectively, whereas the mechanical skin factor is determined from the intercept of the second plot. In addition, a graphical method to determine the reservoir pressure at infinite shut-in time is proposed. Field and simulated tests are presented to demonstrate the applicability of the technique. The results obtained are compared with new, conventional, and pressure derivative type curve matching techniques.

Keywords: buildup; gas well; non-Darcy flow; mechanical skin; permeability; extrapolated shut-in pressure; pseudo-pressure; normalized pseudo-functions

1. Introduction

Gas well tests require additional effort for several theoretical and practical problems that are not normally encountered in oil well tests. The most important problems are: (1) nonlinearity of the diffusivity equation describing real gas flow in the reservoir, (2) the presence of a rate-dependent skin effect around the wellbore of high flow rate wells, and (3) the long wellbore storage period experienced in some low permeability reservoirs.

Many publications that offer solutions for these problems are presented in the literature. The nonlinearity problem was effectively handled by incorporating the pseudo-pressure (Al-Hussainy et al., 1966; Al-Hussainy and Ramey, 1966) and pseudo-time functions into the diffusivity equation (Agarwal, 1979; Lee and Holditch, 1982; Spivey and Lee, 1986).

Practical limitations at the wellsite do not often allow the conduction of a long-term transient test to reach the semilog straight-line period characteristic of a radial reservoir response. Conventional analyses of wellbore-storage-dominated data yield inaccurate, or even no estimates, of reservoir parameters. Type curve matching has been suggested to analyze such

* Corresponding author. Fax: +965-4849558; e-mail: nashawi@petrol.kuniv.edu.kw
[1] Fax: +971-3-632382; e-mail: reyadh@eclsun.uaeu.ac.ae.

0920-4105/98/$19.00
PII S0920-4105(98)00043-6

data. However, type curve matching results may not be unique and hence is best used as a diagnostic tool to determine the reservoir model that matches the well test data (Agarwal et al., 1970a,b; McKinley, 1971a,b; Earlougher et al., 1973). Recently, with enhancements in bottomhole flow rate and pressure recording tools, the focus of both oil and gas well testing has shifted from the time consuming conventional techniques to advanced, and more reliable, convolution (Meunier et al., 1985; Kuchuk and Ayestaran, 1985; Guillot and Horne, 1986; Ahmed et al., 1987; Kuchuk, 1987; Nashawi, 1994) and deconvolution methods (Stewart et al., 1983; Fetkovich and Vienot, 1984; Thompson and Reynolds, 1986; Thompson et al., 1986; Kuchuk, 1990). These new techniques have several advantages over their conventional counterparts, such as minimization of wellbore storage effects, better reservoir description in the vicinity of the wellbore, and accurate estimates of reservoir parameters.

The last problem in the analysis of gas well tests is the presence of turbulent or non-Darcy flow effect in the vicinity of the wellbore. This problem is magnified in high flow rate wells, where it can cause severe pressure drop near the wellbore and may even mask the presence of a fracture. This effect has been traditionally treated as an additional rate-dependent skin. Several techniques have been presented in the literature to determine the rate-dependent or non-Darcy skin effect. Flow-after-flow (Meunier et al., 1987), isochronal (Cullender, 1955a,b), and modified isochronal tests (Aziz, 1967; Brar and Aziz, 1978) are few examples of these effective techniques. These techniques, however, except for the one proposed by Brar and Aziz (1978), require a long-duration test. A trial-and-error procedure has also been proposed for this purpose (Odeh and Jones, 1965a,b); but this procedure is awkward to implement in practice. Meunier et al. (1987) included the wellbore storage dominated data in the test analysis. This technique succeeded in reducing the overall test duration; however, it used a trial-and-error method to determine the rate-dependent skin. Horne and Kucuk (1988) presented a nonlinear computer-automated approach where all the reservoir parameters are simultaneously determined. Although this method can deliver good test results, it is not widely favorable for some of the well test analysts who prefer a graphical representation of the buildup test data. Samaniego and Cinco-Ley (1991) proposed a method that permits a direct estimation of the mechanical skin factor and the turbulent flow coefficient; however, this method is based on a step function approximation of the variable gas flow rate. More recently, Nashawi and Almehaideb (1995) presented a convolution technique that allows the calculation of the reservoir parameters without a trial-and-error procedure; but their analysis relies on the late wellbore storage dominated buildup data when the effect of turbulence dies out.

The objective of this paper is to present a straightforward method that will enable the well test analyst to effectively and accurately determine all reservoir parameters within a short testing period. This study also suggests a method to estimate the extrapolated reservoir pressure at infinite shut-in time from pressure buildup data. Field and simulated tests are employed to illustrate the applicability of the proposed technique.

2. Mathematical model

Meunier et al. (1987) presented a convolution approach to analyze simultaneously measured transient sandface flow rate and pressure buildup data of gas wells under the effects of non-Darcy flow and damage as:

$$\Delta p_{\mathrm{pn}}(\Delta t_{\mathrm{pn}}) = m\left[-\Sigma(\Delta t_{\mathrm{pn}}) + S\Delta q_{\mathrm{D}}\right] + F\Delta q_{\mathrm{D}}^2 \tag{1}$$

Dividing Eq. (1) by Δq_{D} yields:

$$\frac{\Delta p_{\mathrm{pn}}(\Delta t_{\mathrm{pn}})}{\Delta q_{\mathrm{D}}} = m\left[\frac{\Sigma(\Delta t_{\mathrm{pn}})}{\Delta q_{\mathrm{D}}} + S\right] + F(1+q_{\mathrm{D}}) \tag{2}$$

where

$$\Delta p_{\mathrm{pn}}(\Delta t_{\mathrm{pn}}) = p_{\mathrm{pnws}}(\Delta t_{\mathrm{pn}}) - p_{\mathrm{pnwf}} \tag{3}$$

$$\Sigma(\Delta t_{\mathrm{pn}}) = \frac{\Sigma_n}{q_{\mathrm{sc}}} \tag{4}$$

$$\Delta q_{\mathrm{D}} = 1 - q_{\mathrm{D}} \tag{5}$$

$$\Delta q_{\mathrm{D}}^2 = 1 - q_{\mathrm{D}}^2 \tag{6}$$

$$q_D = \frac{q_{sf}(\Delta t_{pn})}{q_{sc}} \tag{7}$$

$$m = \frac{162.6\, q_{sc} B_i \mu_i}{kh} \tag{8}$$

$$S = \log\left(\frac{k}{\phi \mu_i c_{ti} r_w^2}\right) - 3.23 + 0.869 s \tag{9}$$

$$F = 0869 m q_{sc} D \tag{10}$$

The normalized pseudo-pressure and normalized pseudo-time functions are defined, respectively, by:

$$p_{pn} = p_i + \frac{\mu_i}{\rho_i}\int_{p_i}^{p} \frac{\rho(p)}{\mu(p)}\, dp \tag{11}$$

and

$$\Delta t_{pn} = \mu_i c_{ti} \int_0^{\Delta t} \frac{1}{\mu(p) c_t(p)}\, dt \tag{12}$$

The use of normalized pseudo-functions allows the well test analyst to treat gas wells as oil wells provided that the gas flow rate is defined in conventional oil rate units.

In order to isolate the formation permeability and the rate-dependent skin factor from the other unknown parameter, so that they can be calculated independently, Eq. (2) is differentiated with respect to normalized pseudo-shut-in time to obtain:

$$\frac{1}{\Delta q_D^2}\left[\Delta q_D \frac{d\,\Delta p_{pn}(\Delta t_{pn})}{d\,\Delta t_{pn}} + \Delta p_{pn}(\Delta t_{pn}) \frac{dq_D}{d\,\Delta t_{pn}}\right] = m\left\{\frac{1}{\Delta q_D^2}\left[-\Delta q_D \frac{d\Sigma(\Delta t_{pn})}{d\,\Delta t_{pn}} + \Sigma(\Delta t_{pn}) \times \frac{dq_D}{d\,\Delta t_{pn}}\right]\right\} + F\frac{dq_D}{d\,\Delta t_{pn}} \tag{13}$$

Dividing Eq. (13) by the dimensionless flow rate derivative, $dq_D/d\Delta t_{pn}$, yields:

$$\frac{1}{\Delta q_D}\left[\frac{d\,\Delta p_{pn}(\Delta t_{pn})/d\,\Delta t_{pn}}{dq_D/d\,\Delta t_{pn}} + \frac{\Delta p_{pn}(\Delta t_{pn})}{\Delta q_D}\right] = m\left\{\frac{1}{\Delta q_D}\left[-\frac{d\Sigma(\Delta t_{pn})/d\,\Delta t_{pn}}{dq_D/d\,\Delta t_{pn}} + \frac{\Sigma(\Delta t_{pn})}{\Delta q_D}\right]\right\} + F \tag{14}$$

A plot of the left-hand-side of Eq. (14) vs. the term multiplied by m on the right-hand-side of the equation should result in a straight line with slope m and intercept F. Once m and F are determined, the formation permeability, k, and the rate-dependent skin factor, Dq_{sc}, can be calculated from Eqs. (8) and (10), respectively.

The second step involves determining the mechanical skin. To do that, Eq. (2) is rewritten as:

$$1.151\left\{\frac{1}{m}\left[\frac{\Delta p_{pn}(\Delta t_{pn})}{\Delta q_D} - F(1+q_D)\right] - \log\left(\frac{k}{\phi \mu_i c_{ti} r_w^2}\right) + 3.23\right\} = -1.151\frac{\Sigma(\Delta t_{pn})}{\Delta q_D} + s \tag{15}$$

A plot of the left-hand-side of Eq. (15) vs. the sandface rate convolution time function should yield a straight line with the mechanical skin factor as the intercept. For simplicity, the left-hand-side of Eq. (15) will be denoted by S_{tb} in the analysis of the example well tests to be presented later in this study.

Having estimated the formation permeability, the mechanical and the rate-dependent skin factors, the final goal of the proposed technique is to determine the reservoir pressure at infinite shut-in time. Meunier et al. (1985) derived an equation that describes the sandface shut-in pressure of oil wells in an infinite acting reservoir as:

$$p_{ws} = p_i m\left[\log(t_p + \Delta t) + \Sigma(\Delta t) + S q_D\right] \tag{16}$$

Eq. (16) can be modified to fit gas wells by employing the normalized pseudo-functions and by adding the non-Darcy flow effect. In this context, Eq. (16) becomes:

$$p_{pnws} = p_{pni} - \left\{m\left[\log(t_{ppn} + \Delta t_{pn}) + \Sigma(\Delta t_{pn}) + S q_D\right] + F q_D^2\right\} \tag{17}$$

Therefore, the normalized pseudo-pressure at infinite shut-in time of a gas well with turbulence and damage equals the intercept of the straight line obtained by plotting the sandface normalized pseudo-shut-in pressure, p_{pnws}, vs. the term to the right of p_{pni} in Eq. (17). Meunier et al. (1985) called the plot

Table 1
Gas and reservoir properties for simulated case no. 1

Gas properties	
Initial viscosity, μ_i (cp)	0.01877
Initial gas compressibility, C_{gi} (psi^{-1})	0.3028×10^{-3}
Gas specific gravity, SG	0.7
Gas FVF, B_{gi} (bbl/MSCF)	1.087
Well/reservoir properties	
Productive thickness, h (ft)	50
Hydrocarbon porosity, ϕ (%)	12
Wellbore radius, r_w (ft)	0.1667
Reservoir temperature, T (°R)	710
Initial reservoir pressure, p_i (psi)	3000

resulting from Eq. (16) the modified Horner graph. The same terminology will be adapted in this paper.

The procedure outlined above can be also employed with the pseudo-pressure function of Al-Hussainy et al. (1966). The only difference is that the slope of the first plot will be defined as:

$$M=\frac{1637q_{SC}T}{kh} \tag{18}$$

3. Discussion of the working equations

Eq. (13) is general in the sense that it is applicable for the entire duration of the shut-in period as long as the afterflow can be accurately measured. The intent of this equation is to reduce the duration of the buildup test. However, if the test is conducted long enough until the afterflow rate becomes relatively small, 2 phenomenological behaviors can take place. First, the turbulence effect dies out. In such a case, the last term on the right-hand-side of Eq. (13) drops out of the equation because the inertial turbulent flow factor, F, approaches zero. Second, when the afterflow rate decreases the dimensionless flow rate decreases as well and hence, its derivative with respect to time tends toward zero. Thus, taking these effects into consideration, Eq. (13) can be rewritten as follows:

$$\frac{\mathrm{d}\,\Delta p_{pn}(\Delta t_{pn})}{\mathrm{d}\,\Delta t_{pn}}=m\left[-\frac{\mathrm{d}\,\Sigma(\Delta t_{pn})}{\mathrm{d}\,\Delta t_{pn}}\right] \tag{19}$$

Eq. (19) can be expressed in terms of the normalized pseudo-shut-in pressure as:

$$\frac{\mathrm{d}\,p_{pnws}(\Delta t_{pn})}{\mathrm{d}\,\Delta t_{pn}}=m\left[-\frac{\mathrm{d}\,\Sigma(\Delta t_{pn})}{\mathrm{d}\,\Delta t_{pn}}\right] \tag{20}$$

Thus, using the data recorded at the end of the wellbore storage period and plotting the normalized pseudo-shut-in pressure derivative vs. the sandface rate convolution time derivative, a straight line should result. The slope of this line equals the conventional slope m. This type of analysis will only allow the calculation of the formation permeability. To obtain the mechanical and the rate-dependent skin factors Eq. (1) is rearranged as:

$$1.151\left\{\frac{1}{\Delta q_D}\left[\frac{\Delta p_{pn}(\Delta t_{pn})}{m}+\Sigma(\Delta t_{pn})\right]-\log\left(\frac{k}{\phi\mu_i c_{ti} r_w^2}\right)+3.23\right\}=(1+q_D)Dq_{SC}+s \tag{21}$$

Thus, the rate-dependent and the mechanical skin factors are, respectively, determined from the slope and the intercept of the straight line obtained by plotting the left-hand-side of Eq. (21) denoted by Y_{21} vs. $(1+q_D)$.

4. Applications

One field example reported in the literature and 2 simulated cases are employed to illustrate the appli-

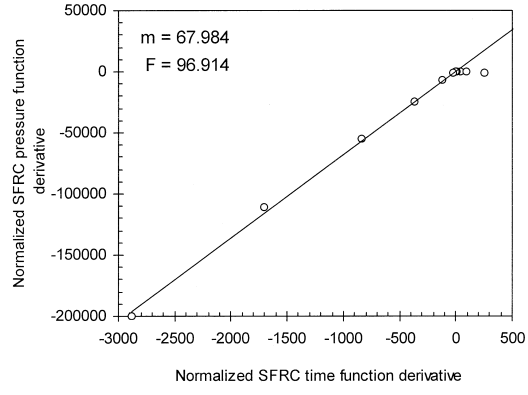

Fig. 1. First test plot: simulated case no. 1.

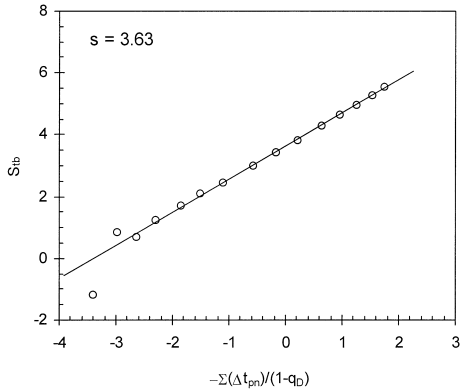

Fig. 2. Second test plot: simulated case no. 1.

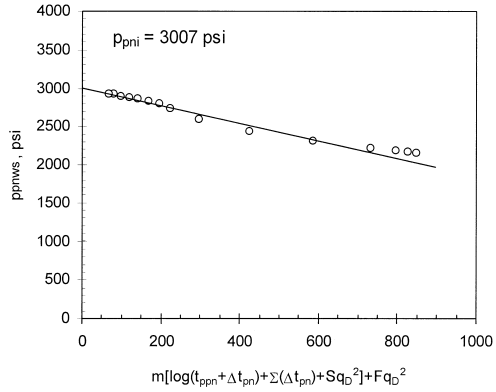

Fig. 4. Modified Horner graph: simulated case no. 1.

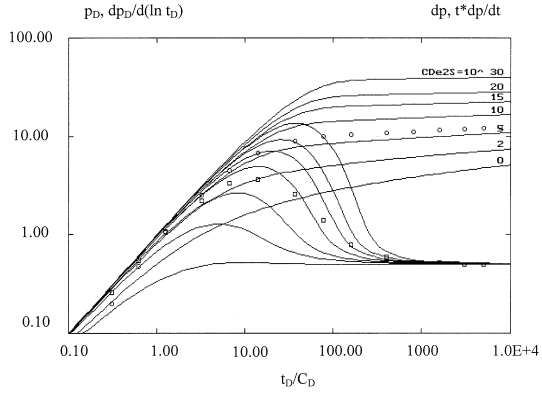

Fig. 3. Type curve matching: simulated case no. 1.

cability of the proposed method. The downhole pressure and flow rate vs. time data for the simulated cases are obtained from an integrated reservoir–wellbore simulator developed by Almehaideb et al. (1989). This model simulates transient flow of oil, water, or gas in the reservoir around a single well that may be opened or closed. Wellbore storage and both mechanical and rate-dependent skin effects are rigorously considered in the model. Flow in the reservoir around the well is radial and the well is assumed to penetrate the whole pay zone.

Although type curve analysis can only deliver values for the formation permeability and the total skin effect, it is implemented in all presented cases for comparison purposes.

4.1. Simulated case no. 1

This case simulates a high-pressure, relatively low-permeability reservoir. The well produced at a flow rate of 5 MMSCF/D for 20 days before it was shut-in to perform a pressure buildup test. The reservoir permeability, and the mechanical and rate-dependent skin factors included in the simulator have the values of 5 md, 4, and 1.5, respectively. The gas and reservoir properties employed in the simulator are reported in Table 1.

Fig. 1 displays the first test plot. The straight line shown in the figure has a slope of 67.984 and an intercept of 96.914. The formation permeability and the rate-dependent skin are calculated from Eqs. (8) and (10) to be 4.88 md and 1.65, respectively.

Table 2
Results of the simulated case no. 1

Analysis technique	Permeability (md)	Mechanical skin	Rate-dependent skin	Total skin
Simulator input data	5.00	4.00	1.50	5.50
This study	4.88	3.63	1.65	5.28
Type curve	4.58	–	–	4.40

Table 3
Gas and reservoir properties for simulated case no. 2

Gas properties	
Initial viscosity, μ_i (cp)	0.02262
Initial gas compressibility, C_{gi} (psi^{-1})	0.1605×10^{-3}
Gas specific gravity, SG	0.7
Gas FVF, B_{gi} (bbl/MSCF)	0.78077
Well/reservoir properties	
Productive thickness, h (ft)	100
Hydrocarbon porosity, ϕ (%)	13
Wellbore radius, r_w (ft)	0.1667
Reservoir temperature, T (°R)	710
Initial reservoir pressure, p_i (psi)	4420

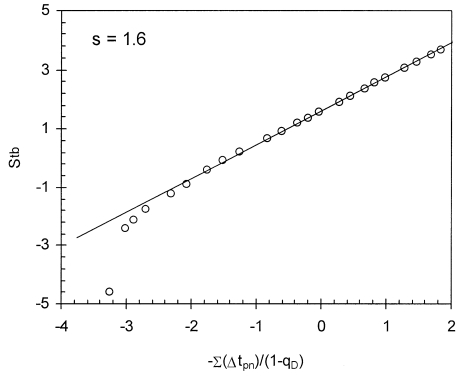

Fig. 6. Second test plot: simulated case no. 2.

Once the slope and the intercept of the first plot are known, the data required for the second test plot are calculated according to Eq. (15). This plot is illustrated in Fig. 2. The mechanical skin factor is equal to the intercept of the straight line drawn through the plotted points and has a value of 3.63, which, when added to the rate-dependent skin, yields a total skin factor of 5.28.

Fig. 3 displays the type curve matching of the data. The analysis yielded a formation permeability of 4.58 md and a total skin factor of 4.4.

Table 2 compares the results for this case. The calculated formation permeability and total skin factor are, respectively, within 2.4% and 4% of the simulator input values. This demonstrates the capability of the presented method in providing good test results.

Fig. 4 illustrates the procedure by which the extrapolated reservoir pressure is estimated. The reservoir pressure equals the intercept of the straight line drawn through all the data points and has a value of 3007 psi. This value falls within 0.2% of the actual value of 3000 psi. Note that the straight line shown in Fig. 4 has a unit slope that is consistent with Eq. (17).

4.2. Simulated case no. 2

The well discussed in this example was producing at a high rate of 20 MMSCF/D before it was closed at the surface. The input reservoir permeability, and the mechanical and rate-dependent skin factors have the values of 10 md, 2, and 4, respectively. Other gas and reservoir properties are presented in Table 3.

The first test plot for this example is displayed in Fig. 5. Least squares method performed on the data

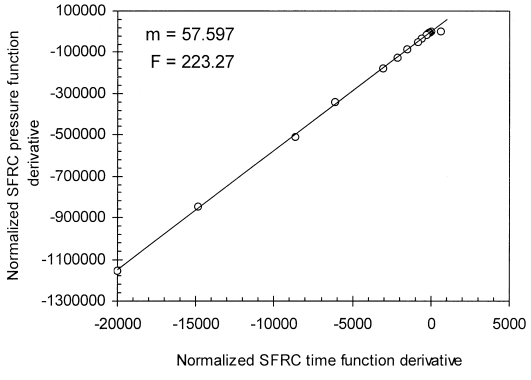

Fig. 5. First test plot: simulated case no. 2.

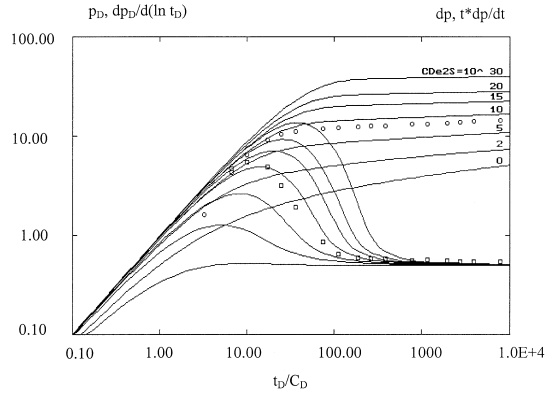

Fig. 7. Type curve matching: simulated case no. 2.

Table 4
Results of the simulated case no. 2

Analysis technique	Permeability (md)	Mechanical skin	Rate-dependent skin	Total skin
Simulator input data	10.00	2.0	4.00	6.00
This study	9.97	1.6	4.46	6.06
Type curve	10.20	–	–	6.30

shows that the straight line drawn in the figure sweeps most of the plotted points and has a slope of 57.597 and intercept of 223.27. The formation permeability and the rate-dependent skin factor were determined as 9.97 md and 4.4, respectively. Fig. 6 illustrates the second test plot. The mechanical skin factor equals the intercept of the line fitted through the data and has a value of 1.6. The total skin factor is calculated to be 6.06.

Type curve analysis conducted on the same data provided a formation permeability of 10.2 md and a total skin factor of 6.3. The type curve matching is shown in Fig. 7.

A comparison of the results is presented in Table 4. As can be noticed, the calculated formation permeability and total skin factor, respectively, fall within 0.3% and 1% of the values used in the simulator. These results further confirm the consistency of the proposed technique in delivering accurate estimates of the reservoir parameters.

The extrapolated reservoir pressure is determined from the modified Horner graph (Fig. 8) and has a value of 4421 psi. This value is within 0.02% of the actual input value of 4420 psi.

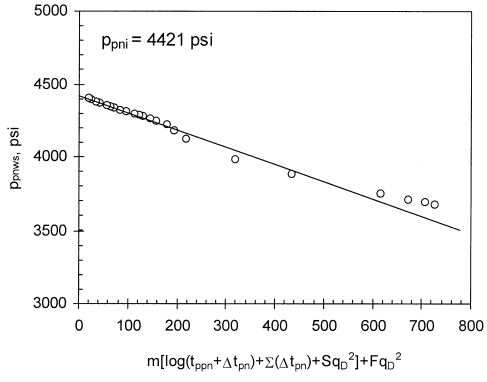

Fig. 8. Modified Horner graph: simulated case no. 2.

4.3. Field example

The tested well, located in Atascosa County, TX, is completed in a low-permeability sandstone formation. The well was producing gas at a flow rate of 480 MSCF/D before it was shut-in for a pressure buildup test. Detailed gas properties, well, and reservoir data are reported in Table 5. Measured and calculated test data are listed in Table 6.

This field example may not be the best candidate to demonstrate the application of the proposed technique. Ahmed et al. (1987) stated that the data of this example have, for unknown reasons, an unusual behavior. This behavior is quite noticeable in the pressure derivative type curve (Fig. 9) that exhibits couple of humps before the slope stabilizes. This trend of the pressure derivative adversely affected the first test plot (Fig. 10) and limited the analysis to

Table 5
Gas and reservoir properties for Ahmed et al. (1987) field example

Gas properties	
Gas viscosity ($t = 0$) (cp)	0.015
Gas specific gravity, SG	0.685
Gas FVF, B_{gi} (bbl/MSCF)	0.13678
Gas compressibility, C_g (psi^{-1})	1.02×10^{-3}
Well/reservoir properties	
Productive thickness, h (ft)	130
Hydrocarbon porosity, ϕ (%)	13
Wellbore radius, r_w (ft)	0.354
Reservoir temperature, T (°R)	712
Pressure ($t = 0$)(psi)	980.62
Production rate (MSCF/D)	480.231
Total producing time (h)	720
Water saturation (%)	28
Water compressibility, C_w (psi^{-1})	2×10^{-6}
Formation compressibility, C_f (psi^{-1})	5×10^{-6}
Total compressibility, C_t (psi^{-1})	1.025×10^{-3}

Table 6
Buildup test data Ahmed et al. (1987) field example

Buildup time (h)	Normalized pseudo-BHP (psi)	Sandface flow rate (MSCF/D)
0.00029364164	980.43671	480.2312440
0.0027936390	981.14709	471.1349095
0.0039047613	981.73773	463.8957411
0.0047380920	982.24860	456.1456847
0.0052936361	982.64941	445.2733051
0.0069603031	984.00323	437.2896410
0.0089047560	985.92145	433.9522614
0.010849209	988.15509	422.2192718
0.013626992	991.70575	415.3305412
0.017515870	997.17413	411.1322050
0.027793648	1013.0222	392.5097614
0.037793640	1029.4829	377.4449681
0.052238077	1053.8849	362.3697614
0.068349212	1081.3345	347.0847050
0.091404766	1120.4108	340.7570230
0.10862699	1149.3829	320.7051296
0.15362701	1223.8276	305.6693913
0.18584922	1276.1522	275.5559220
0.25529370	1385.6702	250.5424271
0.36362699	1544.0752	240.4812581
0.47612703	1690.4066	210.4615912
0.57362705	1803.3966	160.4187184
0.64946043	1882.2963	140.2870068
0.79834926	2011.8174	100.2282342
1.1094604	2198.1550	80.16041935
1.4738492	2355.3201	57.39590340
1.8094047	2467.5828	45.15137695
2.2235715	2589.3755	35.07632845
2.8434603	2740.5979	20.01559650
4.1115160	2937.7834	10.00783630
4.3717937	2965.5786	0
4.9442940	3019.8845	0
5.5909605	3069.1270	0
6.4517937	3117.6331	0
7.2954059	3159.0295	0
8.0251274	3188.8958	0

only few data points between 0.48 and 4.11 h. The data points recorded after 4 h cannot be analyzed using Eqs. (14) and (15) since after this time the flow rate is zero (Table 6). Fortunately, however, this type of data can be analyzed with Eqs. (20) and (21) as it will be illustrated later in the example.

The formation permeability and the rate-dependent skin factor are determined from the straight line displayed in Fig. 10 as 0.062 md and 1.024, respectively. These results are based on 8 data points only.

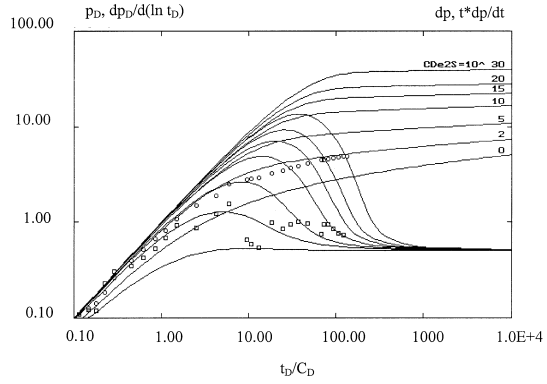

Fig. 9. Type curve matching: Ahmed et al. (1987) field example.

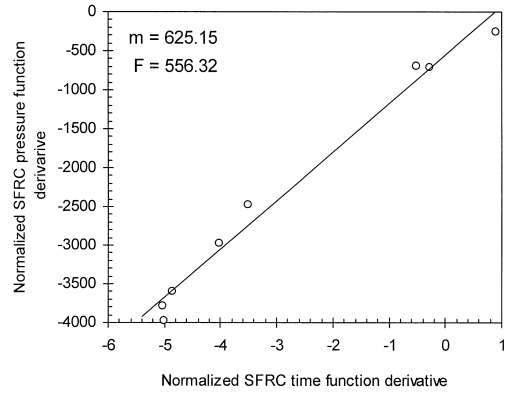

Fig. 10. First test plot: Ahmed et al. (1987) field example.

Fig. 11 shows the second test plot. The mechanical skin factor is determined from the intercept of the straight line to be −0.858. The total skin factor is

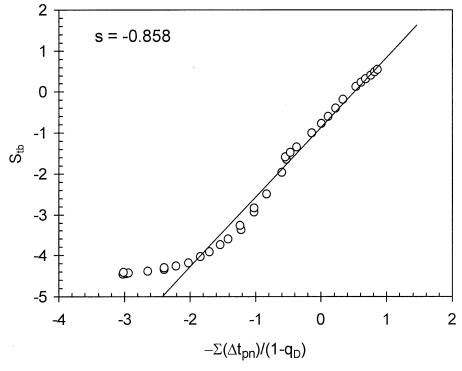

Fig. 11. Second test plot: Ahmed et al. (1987) field example.

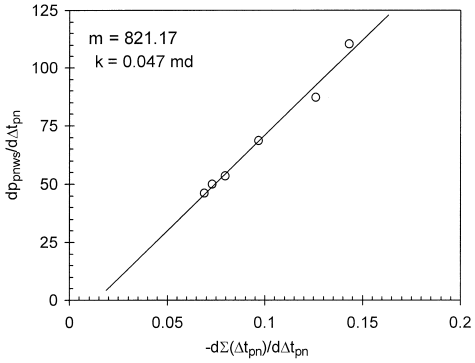

Fig. 12. First test plot using Eq. (20): Ahmed et al. (1987) field example.

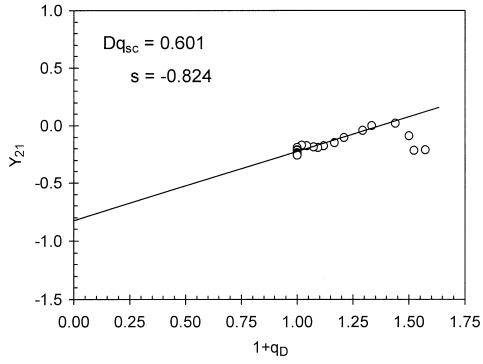

Fig. 13. Second test plot using Eq. (21): Ahmed et al. (1987) field example.

determined to be 0.10. The type curve analysis resulted in a formation permeability of 0.052 md and a total skin factor of −0.05.

As has been mentioned earlier, the last part of the data starting from 4.11 h of the surface shut-in of the well provides the opportunity to demonstrate the applicability of Eqs. (20) and (21) to actual field example. Fig. 12 displays the first test plot using Eq. (20). The formation permeability is determined from the slope of the line shown in the figure to be 0.047 md. Fig. 13 illustrates the second test plot using Eq. (21). The rate-dependent and the mechanical skin factors are, respectively, equal to the slope and intercept of the straight line and have values of 0.601 and −0.824. These results are obtained using data points starting from 0.48 h of buildup.

Ahmed et al. (1987) using convolution, deconvolution, conventional, and type curve matching techniques performed a comprehensive data analysis. These techniques provide an estimate of the total skin factor only, whereas the analysis presented in this paper determines both the mechanical and the rate-dependent skin factors as shown in Table 7. For low productivity wells, as in this field example, the rate-dependent skin is small and does not severely affect the performance of the well. However, for high flow rate wells, non-Darcy flow affects the wells performance and, thus, it must be separately calculated if a good well test analysis is required.

A comparison of the results of this example with Ahmed et al. (1987) results is given in Table 7. The comparison shows that the results obtained in this study are in good agreement with those determined from different analysis techniques by Ahmed et al. (1987). It also shows that the analysis presented here

Table 7
Comparison of results Ahmed et al. (1987) field example

Analysis technique	Permeability (md)	Mechanical skin	Rate-dependent skin	Total skin
This study				
Eqs. (14) and (15)	0.062	−0.858	1.024	0.166
Eqs. (20) and (21)	0.047	−0.824	0.601	−0.222
Type curve	0.052	–	–	−0.050
Ahmed et al. (1987)				
Horner	0.051	–	–	0.59
TRAP	0.047	–	–	0.26
Convolved type curve	0.035	–	–	0.00
Deconvolved type curve	0.048	–	–	0.60
Deconvolved MDH	0.044	–	–	0.50

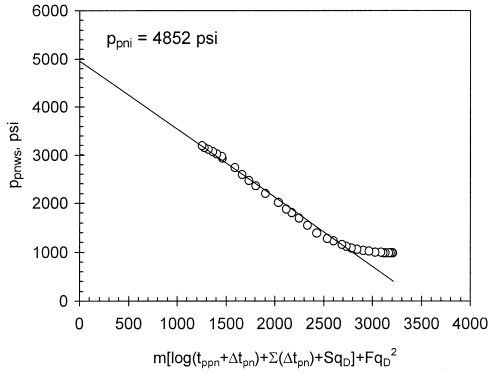

Fig. 14. Modified Horner graph: Ahmed et al. (1987) field example.

has the advantage of providing separate values of the mechanical and the rate-dependent skin factors, whereas the other techniques given in the table do not.

The extrapolated reservoir pressure for this example is obtained from the intercept of the straight line shown in Fig. 14 and has a value of 4852 psi.

5. Conclusions

A direct method is proposed to analyze transient pressure buildup data of gas wells with damage and non-Darcy flow effect. This method employs convolution of the sandface flow rate and pressure data. Its applicability is illustrated through the analysis of 2 simulated cases and 1 field example. The presented method has the following advantages over other methods. (1) The reservoir permeability, mechanical and rate-dependent skin factors are graphically obtained without a trial-and-error procedure. (2) The presented technique utilizes convolution of the early sandface flow rate and pressure test data; thus, allowing accurate description of the reservoir conditions in the vicinity of the wellbore and providing estimates of the reservoir parameters in a short testing time. (3) A graphical method that allows the determination of the extrapolated reservoir pressure has been also presented. The applicability of this method has been illustrated in all analyzed cases. (4) Analysis of the late wellbore storage data is also possible with the proposed method when the effect of non-Darcy flow diminishes. This analysis requires a minor modification of the proposed equations to describe the actual flow rate behavior as it has been demonstrated in the field example.

In order to obtain better analysis results from the presented technique, it is recommend that the downhole pressure and flow rate data be recorded at small time intervals especially early during the well test. Moreover, the accuracy of the first analysis plot is further enhanced when smooth afterflow variations are occurring since derivatives of the recorded data are numerically evaluated in this technique. Any disturbance in the data or unusual pressure behavior may adversely affect the analysis plots.

6. Nomenclature

B_i	initial gas formation volume factor, RB/MSCF
c_t	total system compressibility, psi^{-1}
D	turbulent or non-Darcy flow coefficient, $(MSCF/D)^{-1}$
Dq_{sc}	rate-dependent skin factor, dimensionless
F	inertial turbulent flow factor, Eq. (10)
h	net pay zone thickness, ft
k	formation permeability, md
m	slope of the first test plot, Eq. (8)
M	slope of the first test plot when pseudo-pressure is used, Eq. (18)
p_i	initial reservoir pressure, psi
p_{pni}	normalized pseudo-initial reservoir pressure, psi
p_{pnwf}	normalized pseudo-wellbore flowing pressure, psi
p_{pnws}	normalized pseudo-shut-in pressure, psi
p_{wf}	wellbore flowing pressure, psi
q_D	dimensionless bottomhole rate
q_{sc}	reference flow rate, rate prior to surface shut-in of the well, MSCF/D
q_{sf}	sandface flow rate, MSCF/D
r_w	wellbore radius, ft
s	skin factor
S	skin coefficient term, Eq. (9)
S_{tb}	left-hand-side of Eq. (15), vertical axis of the second test plot
t	production time, h

t_p	Horner production time, h
t_{pn}	normalized pseudo-time, h
t_{ppn}	Horner normalized pseudo-production time, h
Δt	shut-in time, h
Δt_{pn}	normalized pseudo-shut-in time, h
T	formation temperature, °R
Y_{21}	left-hand-side of Eq. (21)

Greek symbols

μ_i	initial gas viscosity, cp
ρ	gas density, lbm/ft^3
Σ	logarithmic approximation of the rate-convolved function, dimensionless
ϕ	formation porosity, fraction

Subscripts

D	dimensionless
i	initial
pn	normalized pseudo-
sc	standard condition
sf	sandface
t	total
w	well
wf	well flowing
ws	well shut-in

Acknowledgements

The authors express their appreciation to Kuwait University Research Administration for financially supporting this work through a university research grant (EP-014).

References

Agarwal, R.G., Al-Hussainy, R., Ramey, H.J., Jr., 1970. An investigation of wellbore storage and skin effects in unsteady liquid flow: I. Analytical treatment. Soc. Pet. Eng. J. (Sept.), 270–290.

Agarwal, R.G., Al-Hussainy, R., Ramey, H.J., Jr., 1970. An investigation of wellbore storage and skin effects in unsteady liquid flow: I. Analytical treatment. Trans. AIME 249.

Agarwal, R.G., 1979. Real gas pseudotime: a new function for pressure buildup analysis of MHF gas wells. SPE 8279, presented at the SPE Annu. Tech. Conf. Exhib., Las Vegas, NV.

Ahmed, U., Kuchuk, F.J., Ayestaran, L., 1987. Short-term transient rate and pressure-buildup analysis of low-permeability reservoirs. SPE Form. Eval. (Dec.), 611–617.

Al-Hussainy, R., Ramey, H.J., Jr., Crawford, P.B., 1966. The flow of real gases through porous media. J. Pet. Technol. (May), 624–636.

Al-Hussainy, R., Ramey, H.J., Jr., 1966. Application of real gas flow theory to well testing and deliverability forecasting. J. Pet. Technol. (May), 637–642.

Almehaideb, R.A., Aziz, K.A., Pedrosa, O.J., Jr., 1989. A reservoir/wellbore model for multiphase injection and pressure transient analysis. SPE 17941, presented at the 6th Middle East Oil Tech. Conf. Exhib., Manama, Bahrain.

Aziz, K., 1967. Theoretical basis of isochronal and modified isochronal back-pressure testing of gas wells. J. Cdn. Pet. Tech. (Jan.–March), 20–22.

Brar, G.S., Aziz, K., 1978. The analysis of modified isochronal tests to predict the stabilized deliverability of gas wells without using stabilized flow data. J. Pet. Technol. (Feb.), 297–304.

Cullender, M.H., 1955. The isochronal performance method for determining the flow characteristics of gas wells. J. Pet. Technol. (Sept.), 137–142.

Cullender, M.H., 1955. The isochronal performance method for determining the flow characteristics of gas wells. Trans. AIME, 204.

Earlougher, R.C., Jr., Kersch, K.M., Ramey, H.J., Jr., 1973. Wellbore effects in injection well testing. J. Pet. Technol. (Nov.), 1244–1250.

Fetkovich, M.J., Vienot, M.E., 1984. Rate normalization of buildup pressure by using afterflow data. J. Pet. Technol. (Dec.), 2211–2224.

Guillot, A.Y., Horne, R.N., 1986. Using simultaneous downhole flow rate and pressure measurements to improve analysis of well tests. SPE Form. Eval. (June), 217–226.

Horne, R., Kucuk, F., 1988. Use of simultaneous flow-rate and pressure measurements to replace isochronal gas well test. SPE Form. Eval. (June), 467–470.

Kuchuk, F.J., Ayestaran, L., 1985. Analysis of simultaneously measured pressure and sandface flow rate in transient well testing. J. Pet. Technol. (Feb.), 323–334.

Kuchuk, F.J., 1987. New methods for estimating parameters of low permeability reservoirs. SPE 16394, presented at the SPE/DOE Symp. Low-Permeability Reservoirs, Denver, CO.

Kuchuk, F.J., 1990. Gladfelter deconvolution. SPE Form. Eval. (Sept.), 285–292.

Lee, W.J., Holditch, S.A., 1982. Application of pseudotime to buildup test analysis of low-permeability gas wells with long-duration wellbore storage distortion. J. Pet. Technol. (Dec.), 2877–2884.

McKinley, R.M., 1971. Wellbore transmissibility from afterflow dominated pressure buildup data. J. Pet. Technol. (July), 863–872.

McKinley, R.M., 1971. Wellbore transmissibility from afterflow dominated pressure buildup data. Trans. AIME, 251.

Meunier, D., Wittmann, M.J., Stewart, G., 1985. Interpretation of pressure buildup test using in situ measurement of afterflow. J. Pet. Technol. (Dec.), 143–152.

Meunier, D.F., Kabir, C.S., Wittmann, M.J., 1987. Gas well test analysis: use of normalized pseudovariables. SPE Form. Eval. (Dec.), 629–636.

Nashawi, I.S., 1994. Short-term analysis technique for pressure buildup test using simultaneously measured transient sandface flow rate and pressure. ADSPE 14, presented at the 6th Abu Dhabi Int. Pet. Exhib. Conf. (ADIPEC) Abu Dhabi, United Arab Emirates.

Nashawi, I.S. Almehaideb, R.A., 1995. A new technique to analyze simultaneous sandface flow rate and pressure measurements of gas wells with turbulence and damage. SPE 29895, presented at the 9th Middle East Oil Show Conf. (MEOS), Manama, Bahrain.

Odeh, A.S., Jones, L.G., 1965. Pressure drawdown analysis, variable-rate case. J. Pet. Technol. (Aug.), 960–964.

Odeh, A.S., Jones, L.G., 1965. Pressure drawdown analysis: variable-rate case. Trans. AIME, 234.

Samaniego V., F., Cinco-Ley, H., 1991. Transient pressure analysis for variable rate testing of gas wells. SPE 21831, presented at the Rocky Mountain Regional Meeting and Low-Permeability Reservoirs Symp., Denver, CO.

Spivey, J.P., Lee, W.J., 1986. The use of pseudotime, wellbore storage, and middle time region. SPE 15229, presented at the SPE Unconventional Gas Technol. Symp., Louisville, KY.

Stewart, G., Meunier, D., Wittmann, M.J., 1983. Afterflow measurement and deconvolution in well analysis. SPE 12174, presented at the SPE Annu. Tech. Conf. Exhib., San Francisco, CA.

Thompson, L.G., Reynolds, A.C., 1986. Analysis of variable-rate well-test pressure data using Duhamel's principle. SPE Form. Eval. (Oct.), 453–469.

Thompson, L.G., Jones, J.R., Reynolds, A.C., 1986. Analysis of pressure buildup data influenced by wellbore phase redistribution. SPE Form. Eval. (Oct.), 435–452.